On-Chip Wavelength Multicasting of 3×320-Gb/s Pulsed-RZ Optical Data

Aleksandr Biberman[(1)], Noam Ophir[(1)], Amy C. Turner-Foster[(2)], Mark A. Foster[(3)], Michal Lipson[(2)], Alexander L. Gaeta[(3)], Keren Bergman[(1)]

[(1)] Department of Electrical Engineering, Columbia University, New York, NY, USA; biberman@ee.columbia.edu
[(2)] School of Electrical and Computer Engineering, Cornell University, Ithaca, NY, USA
[(3)] School of Applied and Engineering Physics, Cornell University, Ithaca, NY, USA

Abstract *We demonstrate for the first time on-chip wavelength multicasting of 320-Gb/s pulsed-RZ data. Using four-wave mixing in a dispersion-engineered silicon waveguide, we perform a 3× multicast, verify full selectivity, perform spectral evaluation, and record eye diagrams for the wavelength-multicasted signal.*

Introduction

Recent advances in silicon photonics have given this integrated platform the potential to enable orders-of-magnitude performance gains in high-performance communication applications, including next-generation optical telecommunication networks, data center interconnection networks, and even photonic networks-on-chip[1]. Endowed with complementary metal-oxide-semiconductor (CMOS) compatibility, silicon-on-insulator (SOI)-based photonic integrated circuits (PICs) are capable of direct integration with advanced microelectronics, with a clear path toward high-volume low-cost mass production.

SOI-based PICs utilizing nonlinear optical processes leveraging four-wave mixing (FWM) have enabled many all-optical functionalities, including wavelength conversion[2], wavelength multicasting[3], spatial multicasting[4], and temporal demultiplexing[5], all on chip. Furthermore, dispersion engineering of these devices enables ultrahigh-bandwidth operation[6].

Future high-performance optical networks will vastly benefit from replacing power-hungry transceivers between nodes with all-optical processes for routing, multicasting, and demultiplexing. Moreover, these processes must sustain the massive bandwidth growth offered by both wavelength-division multiplexing (WDM) and time-division multiplexing (TDM).

Using FWM in highly-nonlinear fiber (HNLF), wavelength multicasting of 320-Gb/s data was recently demonstrated with self-seeded pumps[7]. In this work, we demonstrate on-chip wavelength multicasting of 3×320-Gb/s pulsed-RZ data using a dispersion-engineered silicon waveguide. By selectively toggling the states of the optical input signals, we perform full multicast selectivity, demonstrating all possible states of this 3× multicast. Furthermore, we derive critical performance metrics based on spectral evaluation, and validate the high-speed optical data using eye diagrams.

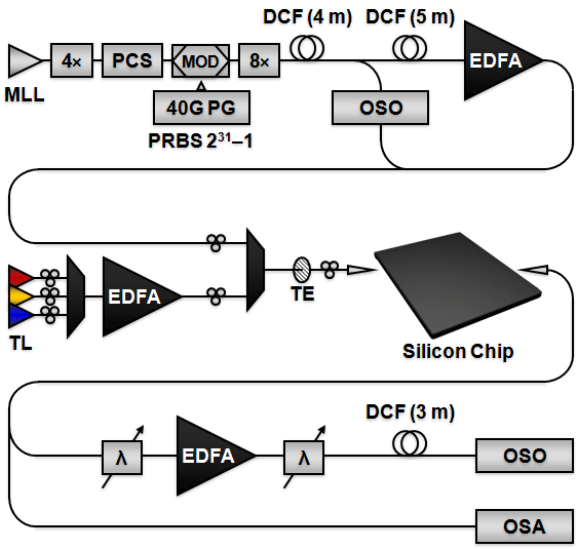

Fig. 1: Diagram of experimental setup used for the 3×320-Gb/s wavelength multicast.

Experimental setup

The dispersion-engineered silicon waveguide in this work has a length of 1.1 cm, height of 290 nm, slab thickness of 25 nm, and width of 720 nm. In the experimental setup using this device, we first generate a 320-Gb/s pulsed-RZ pump signal, combine it with up to three CW wavelength channels, launch the combined signals into the silicon waveguide, and finally extract the signals, examining the resulting wavelength multicasting (Fig. 1). The 320-Gb/s pump signal is generated using a 10-GHz mode-locked laser (MLL), producing 1.5-ps optical pulses, which is first multiplexed to 40 GHz using four-fold (4×) optical time-division-multiplexing (OTDM) stages. The 40-GHz pulse

978-1-4244-8535-2/10/$26.00 ©2010 IEEE

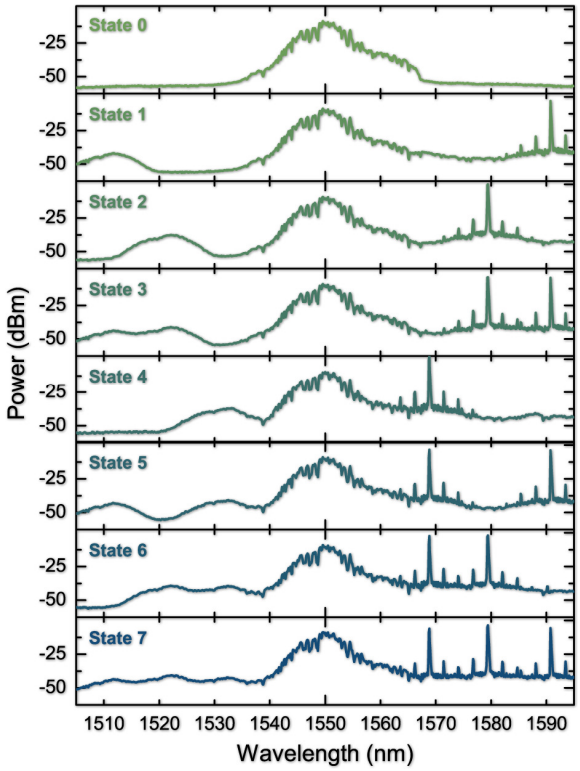

Fig. 2: Output spectra for the resulting signal egressing from the chip for each possible state of the 3×320-Gb/s wavelength multicast. The CW wavelength channels are centered at 1568.8, 1579.4, and 1590.8 nm, the pump signal is centered at 1550 nm, producing wavelength-multicasted wavelength channels centered at 1511.8, 1522.0, and 1532.2 nm. The OSNR in the spectra is limited by the dynamic range of the OSA.

	State 0	State 1	State 2	State 3	State 4	State 5	State 6	State 7
Pump Data Rate (Gb/s)	320							
Pulse Width (fs)	600							
Number of Multicasted Channels	0	1	1	2	1	2	2	3
Conversion Efficiency (dB)	NA	–6.12						
Conversion Bandwidth (nm)	NA	79	57.4	79	36.6	79	57.4	79

Fig. 3: Performance metrics for output spectra of all states of the 3×320-Gb/s wavelength multicast.

stream is then compressed using a pulse compressor (PCS), producing 600-fs pulses, and is then encoded with 40-Gb/s on-off-keyed (OOK) data using an amplitude modulator (MOD), with a 2^{31}–1 pseudo-random bit sequence (PRBS) generated by a pattern generator (PG). The 40-Gb/s signal then passes through eight-fold (8×) OTDM stages, producing the 320-Gb/s data stream for the pump signal, which is then amplified using an erbium-doped fiber amplifier (EDFA). The CW wavelength channels are generated using three multiplexed tunable laser (TL) sources, which are then amplified, and combined with the pump signal. The optical signals are subsequently passed through a fiber polarizer, selecting the TE polarization, and launched into the on-chip nanotapered waveguide through a tapered fiber. Once off chip, the resulting signals are split between two paths: one passes through two tunable grating filters (λ) and a preamplifier, isolating a single wavelength-multicasted wavelength channel that is then evaluated using an optical sampling oscilloscope (OSO); the second path is evaluated using an optical spectrum analyzer (OSA). Polarization controllers are used throughout the setup, as well as varying lengths of dispersion-compensating fiber (DCF) to compensate for the induced chromatic dispersion throughout the experimental setup. Before insertion into the chip, the total average power is 22.0 dBm, total average pump power is 21.8 dBm, and the fiber to-fiber insertion loss is 8 dB.

Experimental validation

We first perform the selective wavelength multicast by selectively toggling on and off the appropriate CW wavelength channels (centered at 1568.8, 1579.4, and 1590.8 nm), cycling through all eight possible states: from *State 0*, with all the CW wavelength channels turned off (producing no multicast), to *State 7*, where all three CW wavelength channels are turned on (producing a 3× multicast, with wavelength-multicasted wavelength channels centered at 1511.8, 1522.0, and 1532.2 nm). The 320-Gb/s pump signal (centered at 1550 nm) remains on for each state.

In each wavelength multicasting state, we record the output sprectrum for the resulting signal egressing from the chip (Fig. 2), and record corresponding performance metrics (Fig. 3). For each state, we first record the number of wavelength-multicasted wavelength channels, ranging from 0 to 3, in *State 0* and *State 7*, respectively. Comparing the spectra, we first observe that the conversion efficiency, defined as the difference in the peak power between the CW wavelength channels and the wavelength-multicasted wavelength channels (both at the

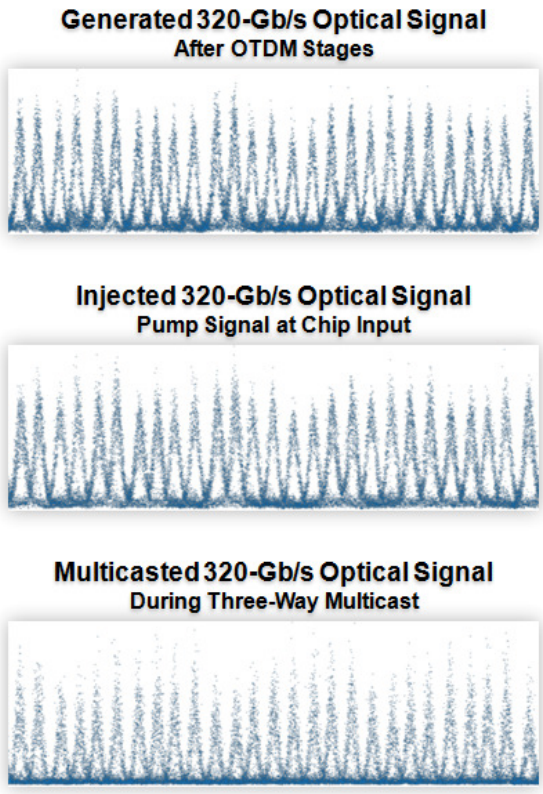

Fig. 4: Eye diagrams of the generated, injected, and wavelength-multicasted (centered at 1532.2 nm) optical signal during the 3×320-Gb/s wavelength multicast. Here, the pulse separation is 3.125 ps.

output of the chip), remains constant at –6.12 dB for each state (except *State 0*, which does not have any wavelength-multicasted wavelength channels). The conversion efficiency value is obtained by comparing the peak power of the CW wavelength channels with the peak power of the wavelength-multicasted wavelength channels, accounting for the 3-dB difference between the observed average power of the entire wavelength-multicasted optical data signal (–19.31 dBm) and the peak power in the modulation, as well as a 7.17-dB difference due to the inherent duty cycle of the 600-ps pulses in the 320-Gb/s signal.

We further examine the conversion bandwidth in each state (Fig. 3). The highest conversion bandwdith of 79 nm is observed for *State 1*, *State 3*, *State 5*, and *State 7*. The lowest conversion bandwidth is 36.6 nm, which is observed for *State 4*. The conversion bandwidth is a critical consideration for these ultrahigh-bandwidth systems that capitalize on both WDM and TDM, with inherent trade-offs between data rate, pulse width, wavelength channel density, conversion bandwidth, and crosstalk.

We subsequently perform a temporal validation of the 320-Gb/s pulsed-RZ signal that is generated using the OTDM stages, injected into the chip as the pump signal, and wavelength-multicasted in the 3× multicast (Fig. 4). We do this by first observing the pulses of the 320-Gb/s signal egressing from the OTDM stages, and record the eye diagram of the pulse stream. We observe an open eye diagram, with a well-balanced pulse amplitude and phase uniformity. We then examine these pulses after the amplification stage, where the eye diagram remains open and the pulses remain blalanced. Lastly, we set the wavelength multicasting in *State 7* (with a 3× multicast), examine the pulses of the wavelength-multicasted wavelength channel centered at 1532.2 nm, and record the eye diagram of this wavelength-multicasted pulse train. Here, we observe open eye diagrams, with noticable degradation in the signal. Most of this degradation is attributed to OSNR degradation in the preamplifier used to recover the wavelength-multicasted signal, rather than the wavelength multicasting process.

Conclusions

Using FWM in a dispersion-engineered silicon waveguide, we demonstrate on-chip wavelength multicasting of 3×320-Gb/s pulsed-RZ data. We verify full wavelength multicasting selectivity using spectral analysis, observing a constant conversion efficiency of –6.12 dB in each configuration, with up to a 79-nm conversion bandwidth. We further observe open eye diagrams for the wavelength-multicasted signal. This demonstrated on-chip wavelength multicasting functionality, performed within this integrated CMOS-compatible platform, represents a critical building block for next-generation high-performance optical networks.

This work was supported in part by the DARPA MTO Parametric Optical Processes and Systems program under contract number W911NF-08-1-0058.

References

1 J. Chan et al., J. Lightwave Technol. **PP**, 1305 (2010).
2 B. G. Lee et al., IEEE Photon. Technol. Lett. **21**, 182 (2009).
3 A. Biberman et al., Proc. OFC'09, OTuI3 (2009).
4 A. Biberman et al., Proc. ECOC'09, P2.27 (2009).
5 H. Ji et al., Proc. OFC'10, PDPC7 (2010).
6 A. C. Turner-Foster et al., Opt. Express **18**, 1904 (2010).
7 C.-S. Brès et al., IEEE Photon. Technol. Lett. **21**, 1002 (2009).